ChemComm

Chemical Communications

ROYAL SOCIETY
OF CHEMISTRY
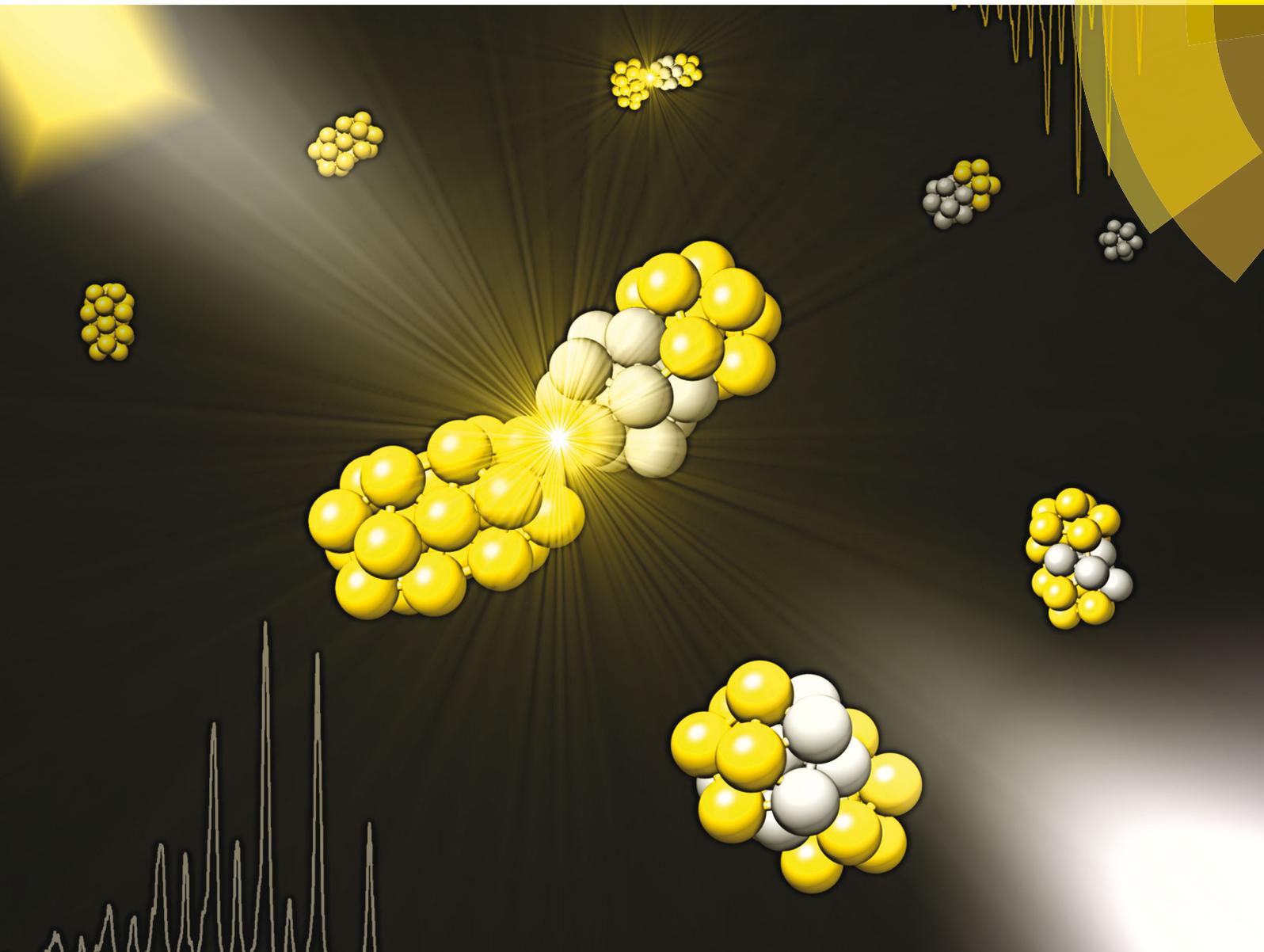
175 YEARS

COMMUNICATION
Thomas Bürgi *et al.*
Silver migration between $Au_{38}(SC_2H_4Ph)_{24}$ and doped $Ag_xAu_{38-x}(SC_2H_4Ph)_{24}$ nanoclusters

COMMUNICATION

Silver migration between Au$_{38}$(SC$_2$H$_4$Ph)$_{24}$ and doped Ag$_x$Au$_{38-x}$(SC$_2$H$_4$Ph)$_{24}$ nanoclusters†

Bei Zhang, Giovanni Salassa and Thomas Bürgi*

A fast redistribution of metal atoms occurs upon mixing the Ag$_x$Au$_{38-x}$ and Au$_{38}$ nanoclusters in solution, as observed by mass spectrometry. Physical separation of Ag$_x$Au$_{38-x}$ and Au$_{38}$ species by a dialysis membrane prohibits the metal migration, which suggests that collisions between the reacting clusters are at the origin of the observation.
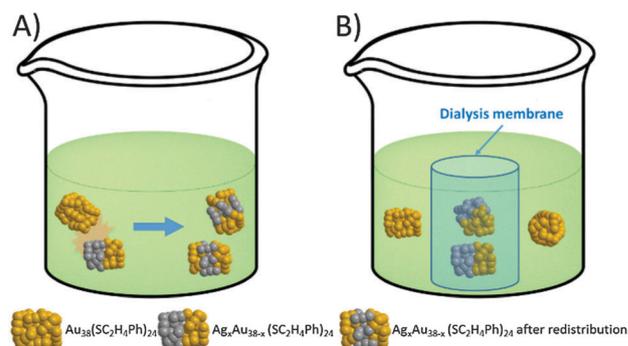
Thiolate protected gold nanoclusters have gained increasing interest due to their precise atomic composition.[1] The structure of the well-defined Au nanoclusters comprises a gold metallic core and protecting SR-(Au–SR)$_n$ staple units. The Au$_{38}$(SC$_2$H$_4$Ph)$_{24}$ nanocluster, for example, is composed of a Au$_{23}$ core, six dimeric staple motifs (SR–Au–SR–Au–SR) and three monomeric staples (SR–Au–SR).[2] The mobility of the thiolates on the cluster surface was evidenced by racemization of the Au$_{38}$ nanocluster enantiomer, which may involve a series of inter-staple S$_N$2-type reactions.[3] In addition, Negishi[4] and Murray[5] both reported an intercluster ligand exchange between gold nanoclusters, suggesting the detachment of ligands or gold–ligand complexes. This is in agreement with older studies on self-assembled monolayers of alkylthiolates on flat gold surfaces, which revealed desorption of radiolabeled thiols into the solution.[6] From recent results in the literature, Au and doped Au clusters seem to be very dynamic systems that are able to easily re-organize themselves.[7,8]

Heteroatoms have been introduced in the core and staples of gold nanoclusters to impart enhanced chemical and physical properties.[9–17] Doping increased the nanocluster surface flexibility and therefore lowered the racemization temperature of chiral Au$_{38}$.[18,19] One of the recently studied methods to obtain bimetallic and trimetallic gold nanoclusters is metal exchange between hetero-metal thiolates and well defined gold nanoclusters.[20,21]

Pradeep and coworkers reported the synthesis of AgAu nanoclusters by instantaneous intercluster metal exchange between Ag$_{44}$(SR)$_{30}$ and Au$_{25}$(SR)$_{18}$ nanoclusters.[22] However, no experimental study has been carried out to address the intercluster metal exchange mechanism. There are two possible pathways: (1) small metal thiolate species (metal A) detach from one nanocluster and attack the other nanocluster (metal B); (2) the two nanocluster exchange metal atoms upon collision.

Here we report the migration of silver atoms between Ag$_x$Au$_{38-x}$ and Au$_{38}$ nanoclusters, which was observed by MALDI mass spectrometry. In order to investigate the metal migration mechanism, a dialysis membrane was applied to separate Ag$_x$Au$_{38-x}$ and Au$_{38}$ nanoclusters spatially (Scheme 1), while allowing the transfer of small species across the membrane. No metal migration occurs under these conditions, pointing towards a collision mechanism for the reaction.

Three batches (denoted A, B and C) of the Ag$_x$Au$_{38-x}$ nanocluster were synthesized by metal exchange between the Au$_{38}$ nanocluster and AgSC$_2$H$_4$Ph (for details see the ESI†). All the three batches showed very similar Ag distribution with

Department of Physical Chemistry, University of Geneva, 30 Quai Ernest-Ansermet, 1211 Geneva 4, Switzerland. E-mail: thomas.buergi@unige.ch

Scheme 1 (A) Reaction between Au$_{38}$(SC$_2$H$_4$Ph)$_{24}$ and Ag$_x$Au$_{38-x}$(SC$_2$H$_4$Ph)$_{24}$ that led to silver migration and consequent redistribution of silver atoms among the clusters. (B) Reaction in the presence of a dialysis membrane that prevent the direct physical contact between Au$_{38}$(SC$_2$H$_4$Ph)$_{24}$ and Ag$_x$Au$_{38-x}$(SC$_2$H$_4$Ph)$_{24}$.
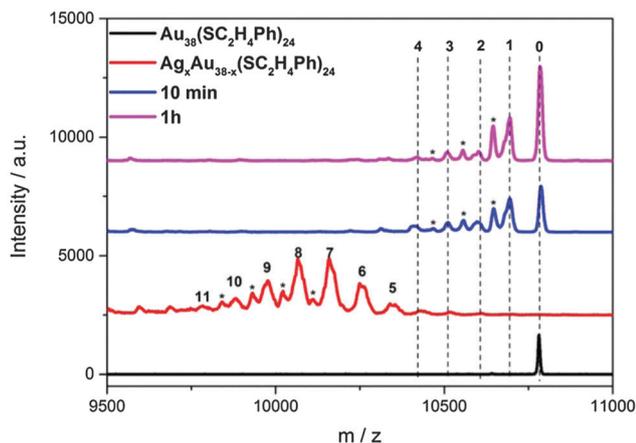
Fig. 1 MALDI spectra of Ag_xAu_{38-x} and Au_{38} nanoclusters, before and after mixing (10 min and 1 h) in solution, silver dopant number x is marked above corresponding peaks. The other peaks belong to loss of a SC_2H_4Ph ($\Delta m/z = 137.2$, marked with an asterisk) during fragmentation. The same fragmentation peaks are also shown in the following MALDI spectra of Au_{38} and Ag_xAu_{38-x}.

species from $x = 3$ to $x = 11$ ("x" being the number of Ag atoms in the cluster). It should be noted that fresh samples were used in this study and multiple passages over a size exclusion column were performed to avoid interference from small species. In the preliminary test, the Ag_xAu_{38-x} nanocluster (batch A) was mixed with Au_{38} in a mass ratio 1 : 1. Upon mixing with Au_{38}, the green solution of Ag_xAu_{38-x} turned brown. Fig. 1 shows the MALDI spectra of starting Ag_xAu_{38-x} and the mixture after 10 minutes and after 1 hour. After 10 minutes, the mixture showed new Ag_xAu_{38-x} species with x around 1 and 2. Meanwhile the starting Ag_xAu_{38-x} clusters with $x > 5$ have disappeared. We calculated the average number of dopant atoms as:

$$\bar{x} = \sum x_i \times A_i / \sum A_i$$

Here A is the corresponding peak area in the MALDI spectra. Upon mixing $\bar{x}$ in the cluster passed from 7.6 to 1.2 only in 10 minutes. The surprisingly low average number of silver atoms after mixing could be due to more pronounced fragmentation of Ag_xAu_{38-x} with a larger x. No significant changes are noted from MALDI spectra after 1 h mixing, indicating that most of the reaction takes place within the first ten minutes.

The UV-vis spectra of Au_{38} and Ag_xAu_{38-x} are clearly different (Fig. S2a, ESI,† compare black and red spectra). In an attempt to follow the evolution of the reaction, UV-vis spectra were collected immediately after the mixing of Ag_xAu_{38-x} (batch B) with Au_{38} and every minute for the following 10 minutes, then one after 20 minutes and 30 minutes. These spectra are reported in Fig. S2b (ESI†). No clear changes were observed in the spectra recorded at different times after the mixing. Difference spectra obtained by subtracting the first spectrum recorded after mixing from all the subsequent spectra (Fig. S2c, ESI†) showed only minor changes. It turned out that the UV-vis spectrum of the product Ag_xAu_{38-x} (with an intermediate $\bar{x}$) could be synthesized by the superposition of the spectra of the original Ag_xAu_{38-x} cluster (with large $\bar{x}$) and Au_{38} (see the fit in the Fig. S3, ESI†).

This means that the absorption spectroscopy is not very sensitive to the migration of metal atoms in this case.

Ag_xAu_{38-x} (batch C, average dopant number $\bar{x} = 6.0$) was mixed with Au_{38} in two mass ratios (Ag_xAu_{38-x} : $Au_{38} = 2 : 1$ and $1 : 1$). The MALDI spectrum (Fig. S4, ESI†) shows that in both cases the distribution of Ag_xAu_{38-x} clusters is shifted to lower x values after mixing with Au_{38}. As expected the mixture containing more silver has a distribution with higher x values.

We furthermore compared the MALDI spectrum of batch B immediately after synthesis and size exclusion and after stirring the sample for three hours. As shown in Fig. S5 (ESI†) the average number of silver atoms remained centred around $x = 6.5$ but the distribution of species with different x became sharper with time. This indicates that metal exchange takes place between Ag_xAu_{38-x} clusters as well. The observed change in compositional distribution reflects a thermodynamic driving force towards a narrower distribution. The narrow distribution indicates that silver incorporation is thermodynamically favoured in specific positions in the Au_{38} cluster, as was evidenced recently by Dass and coworkers.[10] In the latter's work it was shown that silver preferentially occupies nine positions on the cluster core surface. In fact the distribution of species Ag_xAu_{38-x} observed after three hours of stirring (Fig. S5, ESI†) is close to a binomial distribution of 6.4 Ag atoms over nine possible sites (see Fig. S6, ESI†). The same number of silver atoms distributed over 38 sites gives a much broader binomial distribution. This indicates that the system evolves towards a situation where the silver atoms occupy a restricted number of sites in the cluster.

To study the mechanism of this fast Ag migration from Ag_xAu_{38-x} to Au_{38}, experiments were conducted using a dialysis membrane. This allows one to physically separate the two clusters, whereas the transport of small species (<1000 Da) through the membrane is possible. To check the performance of the dialysis membrane a DCM solution of 2-phenylethanethiol (2-PET) was placed inside the membrane and pure DCM was placed outside (the dialysis reaction is denoted as 2-PET|DCM, the same format is applied for the following dialysis study). After dialysis, the outside DCM solution showed the characteristic peaks of 2-PET in ^{1}H-NMR (Fig. S7, ESI†). The same condition was applied for Ag_xAu_{38-x}|DCM and Ag_xAu_{38-x}|Au_{38} (Ag_xAu_{38-x} batch B). After dialysis, the Ag_xAu_{38-x} inside the membrane showed no changes in the distribution of Ag and Au (Fig. 2). Note that in the Ag_xAu_{38-x}|DCM experiment no clusters were found outside the membrane, showing that the clusters are too large to penetrate the pores of the membrane.

In the Ag_xAu_{38-x}|Au_{38} dialysis study, no exchanged species were found in the outside solution (Fig. 3). The concentrated outside solution did not show silver migration products ($x > 0$) after 3 h (Fig. S8, ESI†). In the reference experiment using the same Ag_xAu_{38-x} and Au_{38} solutions but without dialysis membrane migration is proved by MALDI (Fig. 3). These findings show that the mechanism of Ag migration does not involve small species that detach from the Ag_xAu_{38-x} cluster and react with Au_{38}. This suggests a mechanism of metal atom exchange involving collisions between the reacting clusters. In our previous report[19] we showed, using racemization studies, that Ag_xAu_{38-x} has a
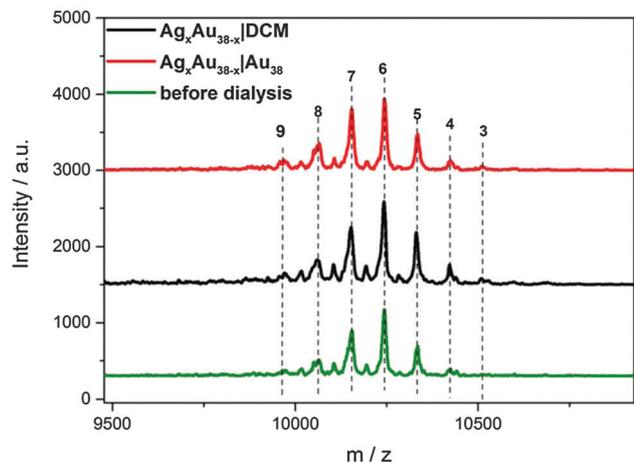
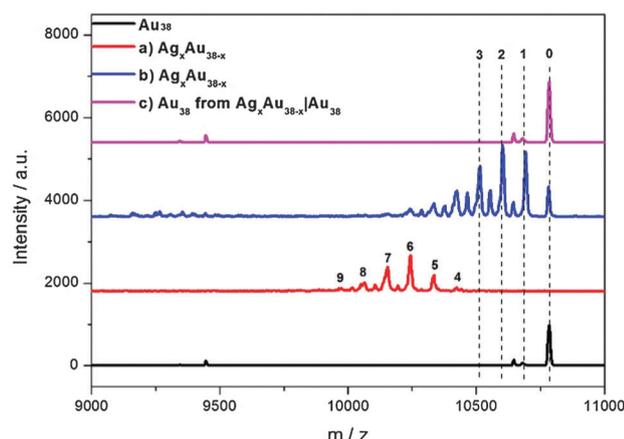Fig. 2 MALDI spectra of Ag_xAu_{38-x}: before and after dialysis experiments.

Fig. 3 MALDI spectra of Au_{38} and Ag_xAu_{38-x}: (a) Ag_xAu_{38-x} before mixing, (b) after mixing Ag_xAu_{38-x} and Au_{38} in solution without the dialysis membrane, (c) Au_{38} outside the dialysis membrane in the $Ag_xAu_{38-x}|Au_{38}$ experiment.

kinetics could be further studied by fluorescence experiments. The distribution of Ag_xAu_{38-x} species with different composition (different x) in solution depends on the starting Ag_xAu_{38-x} and Au_{38} ratio. However, the migration was not detected when the two clusters were physically separated by a dialysis membrane, which allowed small species to diffuse across the membrane. This suggests a mechanism for the metal migration that involves collisions between the reacting clusters. The high flexibility of the Ag_xAu_{38-x} cluster surface, as observed before, may play an important factor in this mechanism.

significantly higher surface flexibility compared to Au_{38} due to the weaker Ag–S bond compared to Au–S. The high flexibility of the Ag_xAu_{38-x} surface may play an important role in the collision mechanism for the metal atom migration observed here. It was proposed earlier[3] that the observed racemization of Au_{38} could take place via inter-staple S_N2-type reactions whereby the staples on the surface of the cluster are mixed among each other. Possibly, metal migration occurs during collision in a similar fashion between clusters therefore mixing staples belonging to different clusters.

In conclusion, silver migration was observed between Ag_xAu_{38-x} and Au_{38} upon mixing in solution. This reaction seems to proceed very fast, on the timescale of minutes, at least. The silver migration

Notes and references

1 H. Häkkinen, *Nat. Chem.*, 2012, **4**, 443–455.
2 H. Qian, W. T. Eckenhoff, Y. Zhu and R. Jin, *J. Am. Chem. Soc.*, 2010, **25**, 8280–8281.
3 S. Knoppe, I. Dolamic and T. Burgi, *J. Am. Chem. Soc.*, 2012, **134**, 13114–13120.
4 Y. Niihori, W. Kurashige, M. Matsuzaki and Y. Negishi, *Nanoscale*, 2013, **5**, 508–512.
5 Y. Song, T. Huang and R. W. Murray, *J. Am. Chem. Soc.*, 2003, **125**, 11694–11701.
6 J. B. Schlenoff, M. Li and H. Ly, *J. Am. Chem. Soc.*, 1995, **117**, 12528–12536.
7 T. Bürgi, *Nanoscale*, 2015, **7**, 15553–15567.
8 W. Kurashige, Y. Niihori, S. Sharma and Y. Negishi, *J. Phys. Chem. Lett.*, 2014, **5**, 4134–4142.
9 R. C. Jin and K. Nobusada, *Nano Res.*, 2014, **7**, 285–300.
10 C. Kumara, K. J. Gagnon and A. Dass, *J. Phys. Chem. Lett.*, 2015, **6**, 1223–1228.
11 B. Zhang, S. Kaziz, H. Li, D. Wodka, S. Malola, O. Safonova, M. Nachtegaal, C. Mazet, I. Dolamic, J. Llorca, E. Kalenius, L. M. Lawson Daku, H. Hakkinen, T. Bürgi and N. Barrabés, *Nanoscale*, 2015, **7**, 17012–17019.
12 B. Molina and A. Tlahuice-Flores, *Phys. Chem. Chem. Phys.*, 2016, **18**, 1397–1403.
13 T. Cesca, B. Kalinic, N. Michieli, C. Maurizio, A. Trapananti, C. Scian, G. Battaglin, P. Mazzoldi and G. Mattei, *Phys. Chem. Chem. Phys.*, 2015, **17**, 28262–28269.
14 F. Muniz-Miranda, M. C. Menziani and A. Pedone, *J. Phys. Chem. C*, 2015, **119**, 10766–10775.
15 S. Wang, X. Meng, A. Das, T. Li, Y. Song, T. Cao, X. Zhu, M. Zhu and R. Jin, *Angew. Chem., Int. Ed.*, 2014, **53**, 2376–2380.
16 G. Soldan, M. A. Aljuhani, M. S. Bootharaju, L. G. Abdulhalim, M. R. Parida, A. H. Emwas, O. F. Mohammed and O. M. Bakr, *Angew. Chem., Int. Ed.*, 2016, **55**, 5749–5753.
17 M. Zhou, J. Zhong, S. X. Wang, Q. J. Guo, M. Z. Zhu, Y. Pei and A. D. Xia, *J. Phys. Chem. C*, 2015, **119**, 18790–18797.
18 N. Barrabes, B. Zhang and T. Burgi, *J. Am. Chem. Soc.*, 2014, **136**, 14361–14364.
19 B. Zhang and T. Burgi, *J. Phys. Chem. C*, 2016, **120**, 4660–4666.
20 S. X. Wang, Y. B. Song, S. Jin, X. Liu, J. Zhang, Y. Pei, X. M. Meng, M. Chen, P. Li and M. Z. Zhu, *J. Am. Chem. Soc.*, 2015, **137**, 4018–4021.
21 S. Yang, S. Wang, S. Jin, S. Chen, H. Sheng and M. Zhu, *Nanoscale*, 2015, **7**, 10005–10007.
22 K. R. Krishnadas, A. Ghosh, A. Baksi, I. Chakraborty, G. Natarajan and T. Pradeep, *J. Am. Chem. Soc.*, 2016, **138**, 140–148.